JACS
JOURNAL OF THE AMERICAN CHEMICAL SOCIETY

Article

pubs.acs.org/JACS

Synthesis and Conformational Dynamics of the Reported Structure of Xylopyridine A

Robert-André F. Rarig, Mai N. Tran, and David M. Chenoweth*

Department of Chemistry, University of Pennsylvania, 231 South 34th Street, Philadelphia, Pennsylvania 19104-6323, United States

Supporting Information

ABSTRACT: Natural products have served as a rich source for the discovery of new nucleic acid targeting molecules for more than half a century. However, our ability to design molecules that bind nucleic acid motifs in a sequence- and/or structure-selective manner is still in its infancy. Xylopyridine A, a naturally occurring molecule of unprecedented architecture, has been found to bind DNA by a unique mode of intercalation. Here we show that the structure proposed for xylopyridine A is not consistent with the characterization in the original isolation report and does not bind B-form DNA. Instead, we report that the originally proposed structure for xylopyridine A represents a new class of conformationally dynamic structure-selective quadruplex nucleic acid binder. The unique molecular conformation locks out nonspecific intercalative binding modes and provides a starting point for the design of a new class of structure-specific nucleic acid binder.

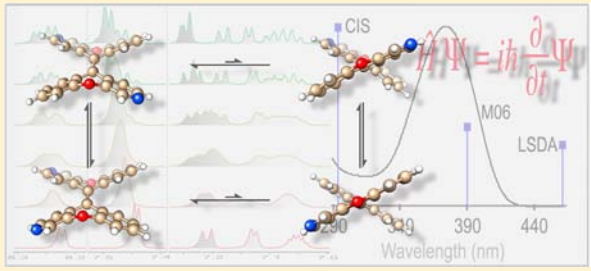

INTRODUCTION

For more than 50 years, natural products have provided a rich source for the discovery of nucleic acid binding molecules, some of which have made far reaching impacts in human medicine ranging from cancer chemotherapy to infectious disease.[1−10] Despite half a century of research, our ability to design small molecules to target nucleic acids in a structure- and sequence-specific manner, beyond the two primary modes of recognition (i.e., intercalation and groove binding) is still in its infancy.[1−14] Targeting DNA and RNA motifs in a structure- and sequence-selective manner allows for small molecule control over cellular events and could provide fundamental insight into biological processes, paving the way for new therapeutic strategies. The development of structure- and sequence-specific small molecule nucleic acid binders represents an important challenge at the frontier of chemical biology, where natural products have historically served as inspiration.[1−14]

Xylopyridine A, a dimeric azaxanthone isolated in 2009 from the mangrove fungus *Xylaria* sp. (#2508), was reported as compound *E*-**1** (Figure 1a) and was found to have potent B-form DNA binding ability.[15−19] Xanthones and azaxanthones are prevalent in natural products, have been shown to bind DNA, and have a rich history in medicinal chemistry with applications in a wide range of therapeutic areas, such as cancer, cardiovascular disease, and infectious diseases.[20−22] Despite this prevalence, the dixanthylidene (reductively dimerized xanthone) architectures have remained elusive in nature until recently.[15−19] The reported diazaxanthylidene structure for xylopyridine A was primarily established using NMR spectroscopy, and its reported optical rotation implied a configurationally stable helically chiral conformation, originally assigned as *E*-twisted on the basis of AM1 calculations.[15] Xylopyridine A was also reported to be emissive, a property used to establish DNA binding using direct fluorimetric titration.[15] The combination of unprecedented natural product architecture, nucleic acid binding ability, and unique conformational properties makes xylopyridine A an important target for synthesis and structural investigations. Motivated by these unique aspects and the possibility of accessing xylopyridine A derivatives, we initiated

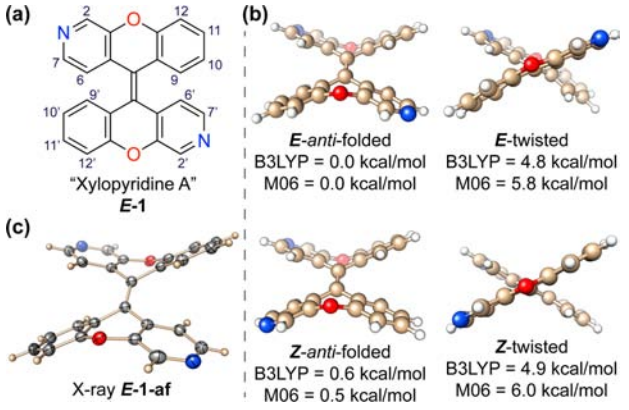

Figure 1. (a) Chemical structure reported for xylopyridine A (*E*-**1**). (b) Relative ground-state free energies calculated using DFT B3LYP and M06 (basis set = 6-311+G(2d,p)) for the *anti*-folded and twisted conformers. (c) X-ray structure of diazaxanthylidene *E*-**1** determined in this report.

Received: May 11, 2013
Published: June 6, 2013

   dx.doi.org/10.1021/ja404737q | *J. Am. Chem. Soc.* 2013, 135, 9213−9219

synthetic studies to shed light on this novel class of nucleic acid binder.

Here, we report the synthesis of the proposed structure for xylopyridine A and show that *E*-**1** is in fact a conformationally dynamic structure with an isomerization barrier accessible at room temperature. X-ray crystallography revealed an *anti*-folded conformation in the solid state (Figure 1c), while DFT calculations and variable temperature NMR studies support a dynamic equilibrating mixture of olefin isomers in solution. Experimental and computational UV−vis spectroscopy data support the minimum energy conformer as *anti*-folded in the solid state and in solution. We show that the structure proposed in the original report of xylopyridine A is not consistent with our analytical data and its true identity remains unresolved. Furthermore, we show that the structure proposed for xylopyridine A is not capable of B-DNA binding. Despite the inability of *E*-**1** to bind B-DNA, we find that a simple modification produces a new class of structure-specific G-quadruplex-binding scaffold that exhibits near perfect specificity over B-form DNA binding.

RESULTS AND DISCUSSION

Prior to initiating synthetic investigations, we used DFT calculations to compare the ground-state structures of the most stable conformers of xylopyridine A (*E*-**1**) and its *Z* isomer (*Z*-**1**).[23] The ground-state structures are shown in Figure 1b, with relative energies using two well-established DFT functionals (see Figure 1b and Supporting Information Table S1). Our calculations predict that the *E*-*anti*-folded conformation is the most stable (0.0 kcal/mol), with the *Z*-*anti*-folded conformation very close in energy (0.5−0.6 kcal/mol). Interestingly, the twisted conformation in both the *E* and *Z* isomers is higher in energy by 4.8−6.0 kcal/mol relative to the *anti*-folded conformers. Based on these calculations, indicating the possibility of an *E*/*Z* mixture in an *anti*-folded conformation, we initiated our synthetic studies.

Given the symmetric nature of xylopyridine A, we envisioned a rapid synthesis of *E*-**1**/*Z*-**1** via reductive homodimerization of 3-azaxanthone **4** (Scheme 1). Our synthesis began with chlorination of commercially available 4-cyanopyridine **2** via lithiation with LiTMP and subsequent treatment with hexachloroethane in THF to afford 3-chloro-4-cyanopyridine. The chloride was displaced using sodium phenoxide in DMF to provide biaryl ether **3**, which was heated to 210 °C in polyphosphoric acid to provide azaxanthone **4** in 56% yield over three steps. Neither McMurry conditions nor Woollins reagent effected efficient homodimerization of **4**. Lawesson's reagent was employed to convert **4** to its corresponding thione **5** in 97% yield.[24] Homodimerization of thione **5** was effected by reductive coupling using copper powder in refluxing toluene[25] to afford **1** as a 1.1:1.0 mixture of *E* and *Z* isomers in 75% yield (Scheme 1). The yield over five steps for *E*-**1**/*Z*-**1** was 41%.

Scheme 1. Synthesis of the Reported Structure for Xylopyridine A

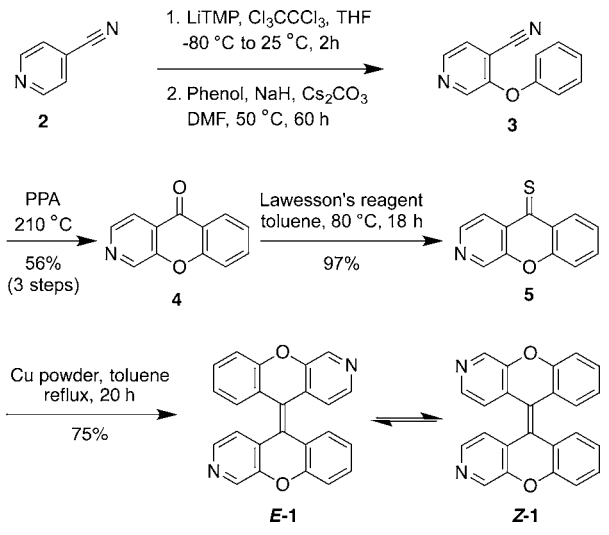

The isomeric mixture of *E*-**1**/*Z*-**1** was inseparable by normal phase, reverse phase, and supercritical fluid chromatography. The mixture was characterized by mass spectrometry (MS), differential scanning calorimetry (DSC), and NMR, UV−vis, fluorescence, and IR spectroscopy. To our surprise, only our MS data were consistent with the characterization data reported for xylopyridine A.[15] The melting point reported for xylopyridine A was 200−202 °C;[15] however, using DSC, we found the melting point of crystalline *E*-**1** to be 327 °C, with decomposition observed above 330 °C (see Supporting Information). A direct NMR comparison was not viable due to the insolubility of *E*-**1** in acetone-d_6 at room temperature. To verify the identity of our dimerization product, single crystals were obtained by slow evaporation from $CHCl_3$/CH_3CN. X-ray data confirmed the structure as *E*-**1** and revealed the *anti*-folded conformation *E*-**1**-af (Figure 1c), which is consistent with the relative ground-state energies from DFT calculations (Figure 1b). Dissolving crystals of *E*-**1** at −10 °C provided a ^{1}H NMR spectrum identical to that of the isomeric mixture, indicating isomer equilibration on an experimentally relevant time scale.

Variable-temperature ^{1}H NMR spectroscopy was used to investigate the dynamic relationship between *Z*-**1** and *E*-**1** (Figure 2).[26] Cooling the sample to −30 °C resulted in sharpening of unresolved doublets at δ 8.26, indicating negligible exchange on the NMR time scale. These doublets are assigned to the pyridine ring and correspond to hydrogens at the 7 and 7′ positions (Figure 1a). Incremental heating up to 50 °C led to signal broadening indicating slow exchange on the

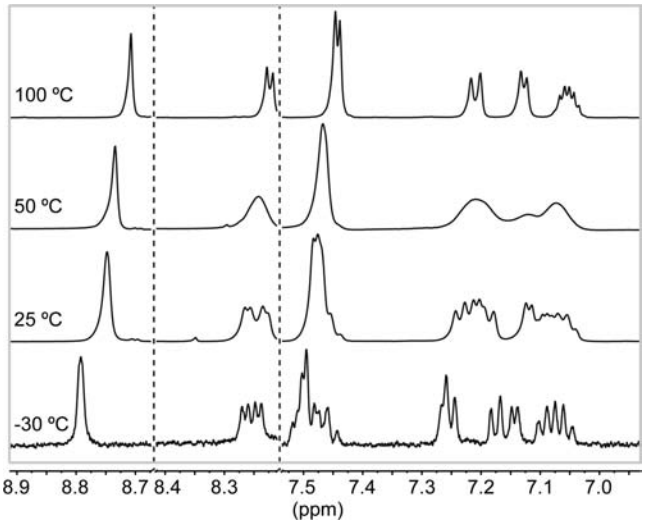

Figure 2. Dynamic NMR showing the temperature-dependent exchange process between isomers *Z*-**1** and *E*-**1**. Variable-temperature NMR experiments conducted in DMF-d_7.

dx.doi.org/10.1021/ja404737q | J. Am. Chem. Soc. 2013, 135, 9213−9219

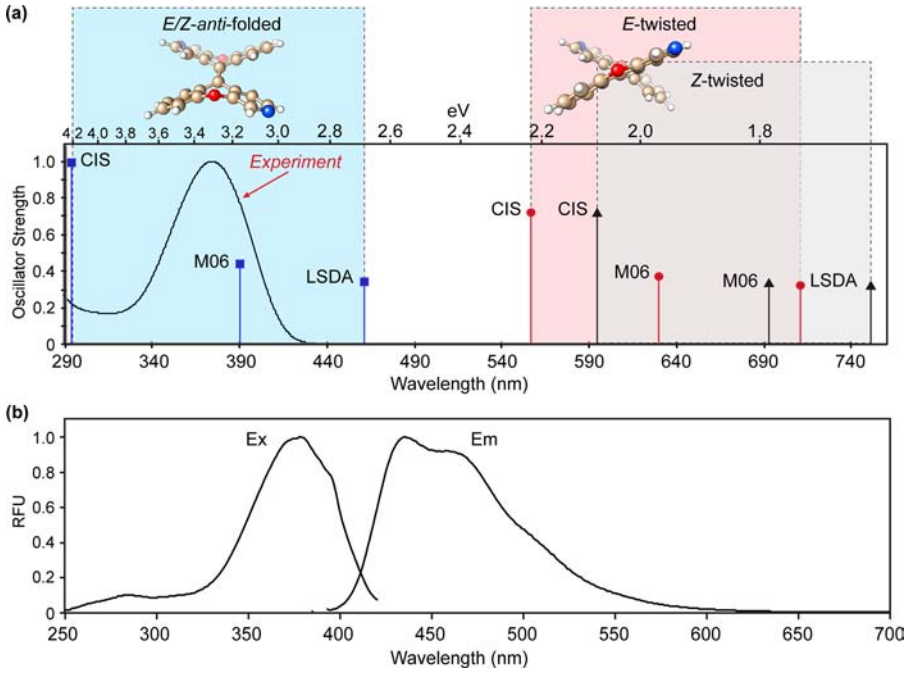

Figure 3. (a) Absorption spectrum overlaid with results from excited state calculations. All excited state calculations were performed with the 6-311+G(2d,p) basis set. The height of each marker corresponds to the oscillator strength at each level of theory. Results for both *E*-**1** and *Z*-**1**, at each level of theory, were less than 0.29 eV (2.4 nm) apart and appear as coincidental lines on the plot above. Absorption data were collected at 23 °C using $CHCl_3$ as the solvent, Abs λ_{max} = 375 nm (ε = 16 659 ± 86 M^{-1} cm^{-1}). (b) Emission and excitation spectra are shown for *E*-**1**/*Z*-**1** in $CHCl_3$ at 23 °C (Em λ_{max} = 435 nm, Ex λ_{max} = 378 nm), and the quantum yield in $CHCl_3$ was found to be Φ = 0.088 ± 0.002.

NMR time scale. Further heating to 100 °C provided a significantly sharpened spectrum due to fast exchange (Figure 2). With a decoupling pulse (3610 Hz) at room temperature, the two doublets at δ 8.26 became two singlets spaced 31.7 Hz apart. Repeating the heating regimen while decoupling allowed for clearer observation of coalescence at 45 °C ($k_{exchange}$ = 70.4 s^{-1}) and fast exchange at 70 °C (see Supporting Information). From the temperature dependent NMR data, the activation energy for the **E-1**/**Z-1** isomerization was determined to be $\Delta G^{\ddagger}$ = 15.9 kcal/mol.

Having established the solid-state structure as the achiral *anti*-folded conformation and the feasibility of a dynamic isomerization process even below room temperature (≤10 °C), we focused our attention on the conformational preference in solution. At this point, all of the data suggested an interconverting mixture of *E*/*Z* isomers in solution. The issue of twisted versus *anti*-folded in solution remained, and we addressed it using a combination of UV−vis spectroscopy and excited state computational methods.[27−31] The experimentally determined absorbance spectrum for *E*-**1**/*Z*-**1** shows a featureless band in $CHCl_3$ with a single maximum at λ_{max} = 375 nm (ε = 16 659 ± 86 M^{-1} cm^{-1}). This is in stark contrast to the reported UV−vis of xylopyridine A, which shows a band with vibronic structure and maxima at λ_{abs} = 376, 398 (λ_{max}), and 425 nm.[15] The possibility of a twisted conformation in solution was evaluated using excited state calculations to simulate the UV−vis spectrum.[32]

Using various levels of theory we were able to bound our experimental result and make a reasonable prediction regarding the presence of the twisted conformation (Figure 3a, Supporting Information Table S2). Levels of theory that span a range of accuracy from overestimating (i.e., CIS)[33,34] to underestimating (i.e., LSDA),[33,34] in addition to putatively more accurate hybrid methods such as B3LYP,[35,36] M06,[37] and range-separated functionals such as ωB97X-D[38] were chosen. Results from theoretical calculations predict the absorption spectrum for the *anti*-folded isomers to be coincidental and centered (at 377 nm) between 4.2 and 2.7 eV (292 and 462 nm). The twisted conformation is predicted to be red-shifted compared to the *anti*-folded conformation by a mean value of nearly 1.6 eV (295 nm) to a range between 555 and 758 nm. Neither the UV absorbance of our synthesized compound (375 nm) nor the λ_{max} of the previously reported species (398 nm) approaches the lower limit (red bounding box, Figure 3a) of the calculated absorbance for the twisted conformation (587 nm). In contrast to the *anti*-folded isomers, the *E* and *Z* forms of the twisted conformation are theoretically differentiated, with the *Z* form predicted to be red-shifted by 0.1 eV (30 nm). Taken together, UV−vis spectroscopy and excited state calculations support a preference for the *anti*-folded conformation in solution. Excitation and emission spectra are shown in Figure 3b, and the quantum yield of *E*-**1**/*Z*-**1** in $CHCl_3$ was found to be Φ = 0.088 ± 0.002.

Xylopyridine A was reported to bind CT-DNA,[15] by intercalation. We found that the structure reported as xylopyridine A (*E*-**1**/*Z*-**1**) did not bind CT-DNA, although solubility was a major impediment in a variety of neutral-to-acidic buffers. Treatment of *E*-**1**/*Z*-**1** with dimethyl sulfate in toluene led to water-soluble *N*-methylpyridinium analogues *E*-**6**/*Z*-**6** (Figure 4a), facilitating nucleic acid binding studies using the equilibrium dialysis method pioneered by Chaires et al.[39−41] The methylated analogues (*E*-**6**/*Z*-**6**) did not bind CT-DNA; however, binding was observed for the human telomeric sequence (Figure 4b), demonstrating that the *anti*-folded diazaxanthylidene architecture can selectively bind quadruplex forming nucleic acid sequences over B-form DNA. This level of selectivity is dramatic compared to the commonly used commercially available quadruplex binder TMPyP4 (cationic

dx.doi.org/10.1021/ja404737q | J. Am. Chem. Soc. 2013, 135, 9213−9219

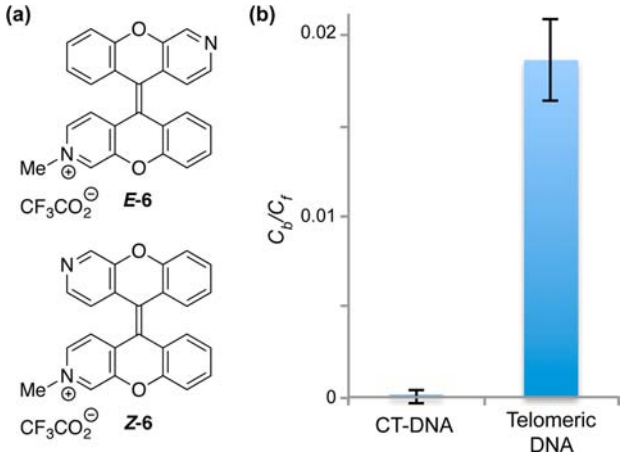

Figure 4. (a) Chemical structure of the *N*-methylpyridinium derivative of *E*-**1**/*Z*-**1**. (b) Results of equilibrium dialysis experiments of *E*-**6**/*Z*-**6** with B-form DNA and telomeric DNA (5′-AGGG(TTAGGG)$_7$-3′). C_b is the bound ligand concentration, and C_f is the free ligand concentration.

porphyrin, 5,10,15,20-tetra(*N*-methyl-4-pyridyl)porphyrin), which only shows a 2.5-fold selectivity for binding telomeric DNA over B-form DNA. Despite considerable debate over the existence and relevance of quadruplexes in vivo, mounting evidence is pointing toward quadruplex nucleic acids as an emerging oncology target.[42,43] Recently, using structure-specific antibodies as probes, Balsubramanian et al. reported results consistent with the observation of quadruplexes in human cells.[44]

The lack of affinity for B-form DNA can be attributed to the lack of planarity caused by the overcrowded *anti*-folded molecular architecture of *E*-**6**/*Z*-**6**. Intercalators are generally planar polyaromatic molecules as exemplified by cryptolepine,[45] which can effectively stack against base-pairs via $\pi-\pi$ stacking interactions. The local unwinding of the nucleic acid helix at an intercalation site results in a translation of the base-pairs along the helix axis a distance equal to the height of an aromatic ring ($h \approx 3.4$ Å, Figure 5b). The *anti*-folded alignment of the nonplanar three-ring systems in *E*-**6**/*Z*-**6** results in a molecular geometry with a height of 5.8 Å, compared to a height of 3.4 Å for a standard intercalator. Within each three-ring system of the *anti*-folded conformer there is an angle of 144° between the corresponding phenyl and pyridyl planes (Figure 5a). This conformation lacks a continuous planar π surface that extends beyond a single six-membered ring, limiting its ability for effective $\pi-\pi$ interactions. The specific stabilizing effects that account for the binding of *E*-**6**/*Z*-**6** with telomeric DNA remain to be determined. However, such specificity compared to B-form DNA binding suggests that this scaffold could serve as a starting point for the design of quadruplex-specific ligands with a novel architecture that locks out nonspecific intercalative binding modes. Future studies focused on targeting unique quadruplex topologies with this new scaffold will be of considerable interest, given its novel architecture.

■ CONCLUSIONS

In summary, the reported structure of xylopyridine A (*E*-**1**) has been synthesized and found to have a low isomerization barrier, allowing for equilibration with its *Z* isomer in solution on an experimentally relevant time scale ($k_{exchange} = 70.4\ s^{-1}$ at 45 °C). Using a combination of experiment and theory, the preferred

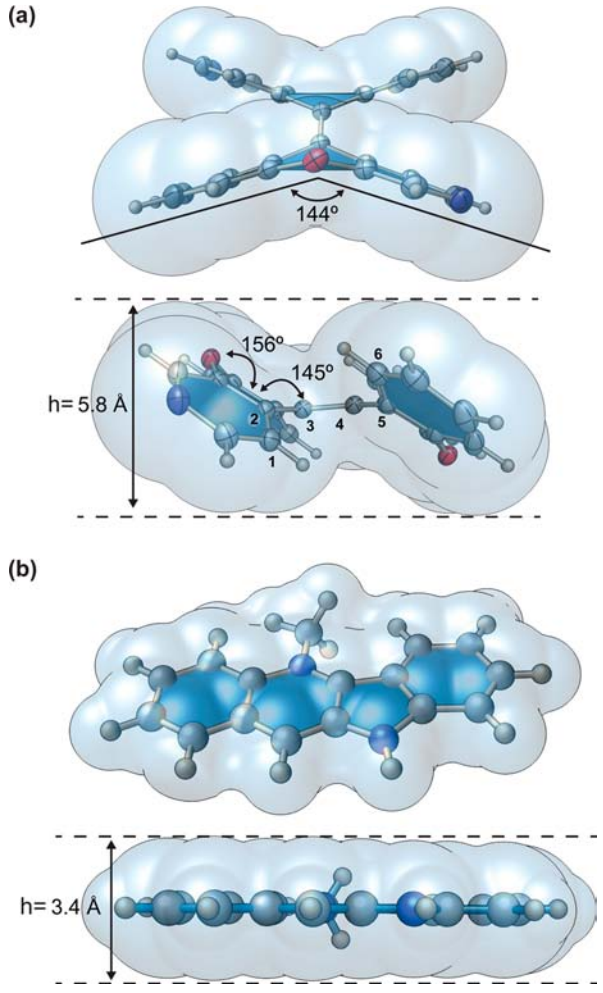

Figure 5. (a) Crystal structure of *E*-**1**, showing a folding angle of 144° between the phenyl and pyridyl planes of each tricyclic system. (b) Crystal structure of the intercalator cryptolepine, showing a planar structure with a height of h = 3.4 Å.

conformation in solution and the solid state was determined to be *anti*-folded. While the identity of xylopyridine A remains unresolved, the synthesis of *E*-**1**/*Z*-**1** has provided a new molecular scaffold for investigating structure-specific nucleic acid binders. The ability to lock out nonspecific B-form DNA intercalation while maintaining affinity for guanine tetrads will be key to the field of quadruplex structure-specific nucleic acid targeting. In depth studies of this new class of conformationally dynamic structure-specific nucleic acid binding scaffold are underway and more details will be reported in due course.

■ EXPERIMENTAL SECTION

General Information. *n*-Butyllithium in hexanes was purchased from Acros and titrated using diphenylacetic acid recrystallized from toluene. All salts used for equilibrium dialysis were purchased from Fisher Bioreagents. The telomeric DNA (5′-AGG GTT AGG GTT AGG GTT AGG GTT AGG GTT AGG GTT AGG G-3′) was purchased from Integrated DNA Technologies. All other reagents were purchased from Sigma Aldrich and used without further purification. Reactions requiring anhydrous conditions were run under argon, using Fisher solvents dried via alumina column. Silica chromatography was done using Silicycle silica gel (55–65 Å pore diameter). Thin-layer chromatography was performed using Sorbent Technologies silica plates (250 μm thickness).

dx.doi.org/10.1021/ja404737q | *J. Am. Chem. Soc.* 2013, 135, 9213–9219

^{1}H and ^{13}C NMR spectra were recorded at 500 and 125 MHz, respectively, on a Bruker UNI 500 ^{1}H NMR. High-resolution mass spectra were obtained by Dr. Rakesh Kohli at the University of Pennsylvania Mass Spectrometry Service Center on a Micromass AutoSpec electrospray/chemical ionization spectrometer. X-ray diffraction structure determination was performed by Dr. Patrick Carroll at the University of Pennsylvania. Infrared spectra were obtained on a Perkin-Elmer BX FT-IR spectrometer. Ultraviolet absorption spectrophotometry was performed on a JASCO V-650 spectrophotometer with a PAC-743R multichannel Peltier using quartz cells with 1 cm cell path lengths. DSC was performed on a TA Instruments Q 2000 differential scanning calorimeter. Reversed-phase column chromatography was performed using a Teledyne Isco CombiFlash Rf system on RediSep Rf Gold C18 columns. High-performance liquid chromatography analysis was carried out using a Jasco HPLC instrument equipped with a Phenomenex column (Luna 5u C18(2) 100A; 250 × 4.60 mm, 5 μm). Equilibrium dialysis experiments were performed in a Thermo Scientific Pierce RED plate with 8K molecular-weight cutoffs.

All calculations were performed using Gaussian 09. All local minima were optimized in the gas phase using DFT-B3LYP and M06 methods with the 6-311+G(2d,p) basis set; they were then confirmed to be stable and to have no imaginary frequencies by stability and frequency calculations, respectively, using the same basis set. All UV−vis calculations were performed using CIS, TD-ωB97X-D, TD-B3LYP, TD-PBEPBE, TD-M06, and TD-LSDA methods with the same basis set in chloroform.

4-Cyano-3-phenoxypyridine (3). In a 50 mL round-bottom flask, phenol (0.809 g, 8.6 mmol) and cesium carbonate (1.645 g, 5.0 mmol) were taken up in DMF (10 mL) and treated with neat sodium hydride (0.339 g, 8.5 mmol). After hydrogen evolution ceased, 3-chloro-4-cyanopyridine[46] (0.583 g, 4.2 mmol) was added neat, and the reaction was stirred at 50 °C for 36 h. Solvent was removed under vacuum, and the crude product was transferred to a separatory funnel with 25 mL of water and 25 mL $CHCl_3$. The aqueous layer was extracted with $CHCl_3$ (three times, 25 mL). The organic layers were combined, washed with 40 mL of 2 N NaOH, dried over $MgSO_4$, concentrated in vacuo, and purified by silica gel chromatography (1:4 EtOAc:hexanes) to provide 4-cyano-3-phenoxypyridine[47] **3** (0.604 g, 3.1 mmol, 73%). ^{1}H NMR (500 MHz, $CDCl_3$): δ 8.46 (1H, d, J = 5 Hz), 8.33 (1H, s), 7.53 (1H, d, J = 5 Hz), 7.46 (2H, dd, J = 7, 9 Hz), 7.28 (1H, t, J = 7 Hz), 7.12 (2H, d, J = 9 Hz).

3-Aza-9*H*-xanthen-9-one (4), Procedure I. Polyphosphoric acid (9.701 g, excess) was added to a beaker containing 4-cyano-3-phenoxypyridine **3**[47] (0.202 g, 1.0 mmol), and the reaction was stirred at 225 °C for 6 h. The reaction was allowed to cool before being diluted with 200 mL of water and slowly basified to pH 7 with solid NaOH. The mixture was transferred to a separatory funnel with 50 mL of DCM, and the aqueous layer was extracted with DCM (three times, 50 mL). The organic layers were combined, dried over $MgSO_4$, concentrated in vacuo, and purified by silica gel chromatography (3:7 EtOAc:hexanes) to provide 3-azaxanthone **4**[48] (0.1679 g, 0.85 mmol, 83%). IR (neat, cm^{-1}): 1682, 1417, 761. ^{1}H NMR (500 MHz, $CDCl_3$): δ 9.01 (1H, s), 8.62 (1H, d, J = 5 Hz), 8.29 (1H, dd, J = 1.5, 8 Hz), 8.06 (1H, d, J = 5 Hz), 7.82−7.72 (1H, m), 7.575 (1H, d, J = 8.5 Hz), 7.40 (1H, t, J = 7.5 Hz). ^{13}C NMR (126.9 MHz, $CDCl_3$): δ 176.6, 156.2, 151.2, 144.5, 142.7, 136.2, 127.1, 126.4, 125.0, 122.4, 118.8, 118.5. HRMS (m/z): $[M + H]^+$ calcd for $C_{12}H_7NO_2$, 198.0555; found, 198.0559.

3-Aza-9*H*-xanthen-9-one (4), Procedure II. A round-bottom flask was charged with 2,2,6,6-tetramethylpiperidine (3.50 mL, 20.7 mmol) and THF (40 mL). The solution was cooled to −30 °C under argon and then treated with 2.38 M n-butyllithium in hexanes (8.34 mL, 19.8 mmol). The solution was allowed to warm to 0 °C and stir for 30 min before being cooled back down to −78 °C. A solution of 4-cyanopyridine **2** (1.030 g, 9.9 mmol) in THF (20 mL) was added over 15 min via syringe pump. After 30 min of stirring at −78 °C, a solution of hexachloroethane (5.000 g, 21.1 mmol) in THF (10 mL) was added over 15 min. After 30 min of stirring at −78 °C, the solution was warmed to room temperature, quenched with saturated NH_4Cl (40 mL), and extracted with ethyl acetate. The combined organic layers were washed with brine, dried over Na_2SO_4, concentrated in vacuo, and run through a short silica plug using 1:1 EtOAc:hexanes to provide crude 3-chloro-4-cyanopyridine[46] (1.196 g). Forty-two percent of this crude product was carried on to the next step.

Phenol (0.692 g, 7.4 mmol), NaH 60% dispersion in mineral oil (0.296 g, 7.4 mmol), Cs_2CO_3 (1.242 g, 3.8 mmol), and DMF (8 mL) were stirred under argon at room temperature. When the bubbling stopped, a solution of the above crude product (0.507 g) in 1 mL of DMF was added, and then rinsed with 1 mL of fresh DMF. After being stirred at 50 °C for 2.5 days, the reaction mixture was allowed to cool to room temperature, quenched with saturated NH_4Cl, and extracted with DCM. The extract was washed with brine, dried with Na_2SO_4, and then concentrated in vacuo to give a brown oil (1.137 g). This oil was transferred to a beaker using a small amount of DCM. After the DCM was removed by stirring at 40 °C, 45 g of polyphosphoric acid was added, and the mixture was stirred at 210 °C overnight. Next, the solution was cooled to room temperature, poured over ice water, and neutralized slowly with concentrated NaOH. The resulting mixture was filtered through Celite and washed with water followed by DCM. The aqueous layer was extracted with DCM. The combined organic layers were washed with brine, dried over Na_2SO_4, and evaporated under reduced pressure to afford 3-azaxanthone[48] **4** as a white solid (0.463 g, 2.3 mmol, 56% over three steps).

3-Aza-9*H*-xanthene-9-thione (5). A mixture of 3-azaxanthone **4** (1.004 g, 5.1 mmol) and Lawesson's reagent (1.257 g, 3.1 mmol) in a 250 mL round-bottom flask was dried at 40 °C under high vacuum for 1 h, and then the flask was back-filled with argon. The mixture was taken up in 160 mL of alumina-dried toluene, heated to 80 °C, and stirred for 18 h. The reaction was concentrated in vacuo, and the crude product was purified by silica gel chromatography (15:85 EtOAc:hexanes) to provide thione **5** as a green solid (1.052 g, 4.9 mmol, 97%). IR (neat, cm^{-1}): 1415, 1330. ^{1}H NMR (500 MHz, $CDCl_3$): δ 9.02 (1H, s), 8.62 (1H, d, J = 8 Hz), 8.55 (1H, d, J = 5 Hz), 8.35 (1H, d, J = 5 Hz), 7.8 (1H, t, J = 8 Hz), 7.52 (1H, t, J = 4 Hz), 7.39 (1H, t, J = 8 Hz). ^{13}C NMR (126.9 MHz, $CDCl_3$): δ 176.6, 156.2, 151.2, 144.5, 142.7, 136.2, 127.1, 126.4, 125.0, 122.4, 118.7, 118.5. HRMS (m/z): $[M + H]^+$ calcd for $C_{12}H_7NOS$, 214.0327; found, 214.0327.

Synthetic Procedure for (*E*/*Z*)-3,3′-Diazaxanthylidene (1). Copper powder (5.133 g, 80.8 mmol) was suspended in toluene (80 mL), 75 mL of which was distilled off to remove water. The distillation apparatus was replaced with a reflux condenser, and the apparatus was flushed with argon before a solution of thione **5** (0.516 g, 2.4 mmol) in 20 mL of toluene was cannulated into the copper suspension. The resulting mixture was heated to 120 °C and stirred for 20 h. The mixture was then gravity filtered, rinsing the copper with 80 °C toluene (100 mL) and boiling $CHCl_3$ (100 mL). The organic fractions were combined, concentrated to dryness, dissolved in the minimum volume of boiling $CHCl_3$, cooled to room temperature, treated with Et_2O (45 mL), and placed in a 4 °C refrigerator for 16 h. Yellow crystalline 3,3′-diazaxanthylidene (*E*-**1**/*Z*-**1**) (0.198 g, 0.6 mmol, 45%) was recovered via Buchner funnel filtration and rinsing with Et_2O. Purification of the mother liquor by silica gel chromatography (3:2 EtOAc:hexanes) provided additional 3,3′-diazaxanthylidene **1** (0.134 g, 0.4 mmol, 30%) as a yellow powder. IR (neat, cm^{-1}): 1410, 1205, 756. ^{1}H NMR (500 MHz, acetone-d_6): δ 8.69 and 8.68 (4H, overlapping singlets), 8.23 and 8.20 (4H, overlapping doublets, J = 5 and 5 Hz), 7.46−7.40 (8H, m), 7.26−6.99 (12H, m). ^{1}H NMR (500 MHz, $CDCl_3$): δ 8.71 and 8.70 (4H, overlapping singlets), 8.21 and 8.17 (4H, overlapping doublets, J = 5 and 5 Hz), 7.38−7.29 (8H, m), 7.19−7.13 (4H, m), 7.07- 7.04 (4 H, m), 7.00−6.92 (4H, m). ^{1}H NMR (500 MHz, DMF-d_7): δ 8.75 (4H, bs), 8.29−8.20 (4H, m), 7.52−7.42 (8H, m), 7.28−7.00 (12H, m). ^{1}H NMR (500 MHz, 3:1 DMF-d_7:F_3CCO_2D): δ 9.35 (4H, bs), 6.9 (4H, dd, J = 5.5, 11 Hz), 8.13 (2H, d, J = 5.5 Hz), 7.87 (2H, d, J = 6 Hz), 7.59−7.49 (8H, m), 7.45 (2H, d, J = 8 Hz), 7.29 (2H, d, J = 8 Hz), 7.18−7.12 (4H, m). ^{13}C NMR (126.9 MHz, $CDCl_3$): δ 162.2, 162.0, 154.8, 154.6, 138.7, 138.2, 138.2, 137.7, 135.2, 134.1, 131.6, 131.3, 128.3, 128.0, 125.1, 124.7, 124.5, 122.9, 122.9, 121.3, 120.8, 18.0, 117.8. HRMS (m/z): $[M + H]^+$ calcd for $C_{24}H_{14}N_2O_2$, 363.1134; found, 214.0327.

dx.doi.org/10.1021/ja404737q | J. Am. Chem. Soc. 2013, 135, 9213−9219

(*E*/*Z*)-*N*-Methyl-3,3′-diazaxanthylidene (6). In a two-necked round-bottom flask, 3,3′-diazaxanthylidene (0.041 g, 0.11 mmol) was suspended in toluene (20 mL). Next, a solution of dimethyl sulfate 1% in toluene (0.53 mL, 0.055 mmol) was slowly added. After a 12 h reflux, the mixture was charged with another batch of dimethyl sulfate 1% in toluene (0.53 mL, 0.055 mmol) and refluxed for 24 h before cooling to room temperature. The mixture was filtered, and the solid was washed several times with toluene and then dissolved in water. The desired product was isolated using reversed-phase column chromatography with 0.1% TFA/water and acetonitrile as eluents (0.030 g, 0.06 mmol, 55%). IR (neat, cm^{-1}): 1693, 1200. ^1H NMR (500 MHz, D_2O): δ 9.06 and 9.03 (2H, overlapping singlets), 8.91 (2H, s), 8.41−8.31 (4H, m), 7.82−7.66 (4H, m), 7.62−7.49 (8H, m), 7.35−7.22 (4H, m), 7.22−7.10 (4H, m), 4.45 and 4.43 (6H, overlapping singlets). ^{13}C NMR (126.9 MHz, D_2O): δ 163.1 163.1, 162.8, 162.6, 162.3, 154.1, 153. 8, 153.8, 153.4, 153.1, 152.4, 152.4, 152.4, 152.3, 139.5, 1 39.2, 139.0, 138.6, 138.5, 137.8, 138.8, 136.7, 136.5, 135.1, 134.0, 131.8, 131.8, 131.3, 127.5, 127.4, 127.3, 125.4, 12 5.2, 125.0, 124.9, 124.8, 124.6, 123.9, 123.1, 123.0, 121.8, 121.3, 120.0, 120.0, 119.4, 119.4, 118.0, 117.6, 117.6, 117. 5, 115.3, 48.2, 48.1. HRMS (m/z): $[M]^+$ calcd for $C_{25}H_{17}N_2O_2^+$, 377.1290; found, 377.1286.

Equilibrium Dialysis Experiments. All experiments were carried out in triplicate using a buffer containing 6 mM Na_2HPO_4, 2 mM NaH_2PO_4, 1 mM Na_2EDTA, and 200 mM NaCl (pH 7). The concentrations of ligand (*E*-**6**/*Z*-**6**) and nucleic acids were determined by UV spectroscopy (260 nm for CT-DNA and telomeric DNA and 410 nm for the ligand).

CT-DNA was dissolved in buffer, followed by dilution to 100 μM (calculated in terms of base pairs). Telomeric DNA was dissolved in buffer, heated to 90 °C, cooled slowly to room temperature, and diluted to 30 μM (in terms of G-quartets). The ligand was dissolved in buffer and diluted to 8 μM.

For each experiment, 500 μL of nucleic acid solution was added to the sample chamber, and 750 μL of ligand solution was added to the buffer chamber. The equilibrium dialysis plate was then covered with a sealing film and incubated at room temperature for 24 h. After incubation, 360 μL of each sample was added to 40 μL of 10% SDS and measured by UV spectroscopy to determine the concentrations of nucleic acids and ligands. Appropriate corrections were made for the dilution resulting from the addition of SDS solution. The free ligand concentration (C_f) was obtained from the buffer chamber, while the total ligand concentration (C_t) was determined from the sample chamber. The bound ligand concentration (C_b) was then calculated: $C_b = C_t - C_f$. The concentration of nucleic acids was also determined from the sample chamber. The ratio C_b/C_f was divided by the concentration of nucleic acids in term of monomeric units (base pairs for CT-DNA and quartets for telomeric DNA). The obtained values were then plotted to demonstrate the selectivity of ligand toward telomeric DNA.

■ ASSOCIATED CONTENT

Ⓢ Supporting Information

Characterization data for all new compounds, X-ray crystallographic data (CIF), and computational details. This material is available free of charge via the Internet at http://pubs.acs.org.

■ AUTHOR INFORMATION

Corresponding Author

dcheno@sas.upenn.edu

Notes

The authors declare no competing financial interest.

■ ACKNOWLEDGMENTS

We thank Drs. George Furst and Rakesh Kohli for assistance in obtaining high-resolution NMR and mass spectral data, respectively, Pat Carroll for X-ray crystallographic assistance, and Joseph Subotnik for helpful discussions regarding excited state calculations. This work was supported by funding from the University of Pennsylvania. We thank the Vietnam Education Foundation for funding (VEF Fellowship to M.N.T.) and the NSF for support of the X-ray diffractometer (Grant CHE-0840438).

■ REFERENCES

(1) Demeunynck, M.; Bailly, C.; Wilson, W. D. *DNA and RNA binders: from small molecules to drugs*, Vols. 1 and 2; Wiley-VCH: Weinheim, 2003.

(2) Hurley, L. H. *Nat. Rev. Cancer* **2002**, *2*, 188−200.

(3) Vicens, Q.; Westhof, E. *ChemBioChem* **2003**, *4*, 1018−1023.

(4) Hermann, T. *Curr. Opin. Struct. Biol.* **2005**, *15*, 355−366.

(5) Carlson, C. B.; Stephens, O. M.; Beal, P. A. *Biopolymers* **2003**, *70*, 86−102.

(6) Palchaudhuri, R.; Hergenrother, P. J. *Curr. Opin. Biotechnol.* **2007**, *18*, 497−503.

(7) Thomas, J. R.; Hergenrother, P. J. *Chem. Rev.* **2008**, *108*, 1171−1224.

(8) Poehlsgaard, J.; Douthwaite, S. *Nat. Rev. Microbiol.* **2005**, *3*, 870−881.

(9) Hartley, J. A.; Hochhauser, D. *Curr. Opin. Pharmacol.* **2012**, *12*, 398−402.

(10) Wilson, W. D.; Tanious, F. A.; Mathis, A.; Tevis, D.; Hall, J. E.; Boykin, D. W. *Biochimie* **2008**, *90*, 999−1014.

(11) Dervan, P. B. *Bioorg. Med. Chem.* **2001**, *9*, 2215−2235.

(12) Neidle, S. *Nat. Prod. Rep.* **2001**, *18*, 291−309.

(13) Guan, L.; Disney, M. D. *ACS Chem. Biol.* **2012**, *7*, 73−86.

(14) Chenoweth, D. M.; Meier, J. L.; Dervan, P. B. *Angew. Chem., Int. Ed.* **2013**, *52*, 415−418.

(15) Xu, F.; Pang, J.; Lu, B.; Wang, J.; Zhang, Y.; She, Z.; Vrijmoed, L. L. P.; Gareth Jones, E. B.; Lin, Y. *Chin. J. Chem.* **2009**, *27*, 365−368.

(16) Jiang, M.-Y.; Feng, T.; Liu, J.-K. *Nat. Prod. Rep.* **2001**, *28*, 783−808.

(17) Zhou, Z.-Y.; Liu, J.-K. *Nat. Prod. Rep.* **2010**, *27*, 1531−1570.

(18) Rateb, M. E.; Ebel, R. *Nat. Prod. Rep.* **2011**, *28*, 290−344.

(19) Xu, J. *Curr. Med. Chem.* **2011**, *18*, 5224−5266.

(20) Pouli, N.; Marakos, P. *Anti-Cancer Agents Med. Chem.* **2009**, *9*, 77−98.

(21) Hansen, M.; Lee, S.-J.; Cassady, J. M.; Hurley, L. H. *J. Am. Chem. Soc.* **1996**, *118*, 5553−5561.

(22) Shen, R.; Wang, P.; Tang, N. *J. Fluoresc.* **2010**, *20*, 1287−1297.

(23) Frisch, M. J.; Trucks, G. W.; Schlegel, H. B.; Scuseria, G. E.; Robb, M. A.; Cheeseman, J. R.; Scalmani, G.; Barone, V.; Mennucci, B.; Petersson, G. A.; Nakatsuj, H.; Caricato, M.; Li, X.; Hratchian, H. P.; Izmaylov, A. F.; Bloino, J.; Zheng, G.; Sonnenberg, J. L.; Hada, M.; Ehara, M.; Toyota, K.; Fukuda, R.; Hasegawa, J.; Ishida, M.; Nakajima, T.; Honda, Y.; Kitao, O.; Nakai, H.; Vreven, T. Montgomery, J. A.Jr.; Peralta, J. E.; Ogliaro, F.; Bearpark, M.; Heyd, J. J.; Brothers, E.; Kudin, K. N.; Staroverov, V. N.; Kobayashi, R.; Normand, J.; Raghavachari, K.; Rendell, A.; Burant, J. C.; Iyengar, S. S.; Tomasi, J.; Cossi, M.; Rega, N.; Millam, J. M.; Klene, M.; Knox, J. E.; Cross, J. B.; Bakken, V.; Adamo, C.; Jaramillo, J.; Gomperts, R.; Stratmann, R. E.; Yazyev, O.; Austin, A. J., Cammi, R.; Pomelli, C.; Ochterski, J. W.; Martin, R. L.; Morokuma, K.; Zakrzewski, V. G.; Voth, G. A.; Salvador, P.; Dannenberg, J. J.; Dapprich, S.; Daniels, A. D.; Farkas, Ö., Foresman, J. B.; Ortiz, J. V.; Cioslowski, J.; Fox, D. J. *Gaussian 09*, revision B.01; Gaussian, Inc.: Wallingford, CT, 2010.

(24) Biedermann, P. U.; Stezowski, J. J.; Agranat, I. *Chem.—Eur. J.* **2006**, *12*, 3345−3354.

(25) Levy, A.; Biedermann, P. U.; Cohen, S.; Agranat, I. *J. Chem. Soc., Perkin Trans.* **2000**, *2*, 725−735.

(26) Sandström, J. *Dynamic NMR Spectroscopy*; Academic Press: London, 1982.

(27) Jacquemin, D.; Mennucci, B.; Adamo, C. *Phys. Chem. Chem. Phys.* **2011**, *13*, 16987−16998.

(28) Casida, M. E.; Huix-Rotllant, M. *Annu. Rev. Phys. Chem.* **2012**, *63*, 287−323.
(29) Adamo, C.; Jacquemin, D. *Chem. Soc. Rev.* **2013**, *42*, 845−856.
(30) Jacquemin, D.; Bremond, E.; Planchat, A.; Ciofini, I.; Adamo, C. *J. Chem. Theory Comput.* **2011**, *7*, 1882−1892.
(31) Fabian, J. *Dyes Pigm.* **2010**, *84*, 36−53.
(32) Marques, M. A. L.; Ullrich, C. A.; Nogueira, F.; Rubio, A.; Burke, K.; Gross, E. K. U. *Time-Dependent Density Functional Theory, Lecture Notes in Physics*, Vol. *706*; Springer: New York, 2006.
(33) Goerigk, L.; Grimme, S. *J. Chem. Phys.* **2010**, *132*, 184103−184111.
(34) Subotnik, J. E. *J. Chem. Phys.* **2011**, *135*, 71104−71107.
(35) Becke, A. D. *J. Chem. Phys.* **1993**, *98*, 5648−5652.
(36) Stephens, P. J.; Devlin, F. J.; Chabalowski, C. F.; Frisch, M. J. *J. Phys. Chem.* **1994**, *98*, 11623−11627.
(37) Zhao, Y.; Truhlar, D. G. *Theor. Chem. Acc.* **2008**, *120*, 215−241.
(38) Chai, J.-D.; Head-Gordon, M. *Phys. Chem. Chem. Phys.* **2008**, *10*, 6615−6620.
(39) Ragazzon, P. A.; Garbett, N. C.; Chaires, J. B. *Methods* **2007**, *42*, 173−182.
(40) Ragazzon, P.; Chaires, J. B. *Methods* **2007**, *43*, 313−323.
(41) Weidemann, T.; Seifert, J.-M.; Hintersteiner, M.; Auer, M. *J. Comb. Chem.* **2010**, *12*, 647−654.
(42) Balasubramanian, S.; Hurley, L. H.; Neidle, S. *Nat. Rev.* **2011**, *10*, 261−275.
(43) Bochman, M. L.; Paeschke, K.; Zakian, V. A. *Nat. Rev.* **2012**, *13*, 770−780.
(44) Biif, G.; Tannahill, D.; McCafferty, J.; Balasubramanian. *Nature Chem.* **2013**, *5*, 182−186.
(45) Lisgarten, J. N.; Coll, M.; Portugal, J.; Wright, C. W.; Aymami, J. *Nat. Struct. Biol.* **2002**, *9*, 57−60.
(46) 1.Cailly, T.; Fabis, F.; Lemaitre, S.; Bouillon, A.; Rault, S. *Tetrahedron Lett.* **2005**, *46*, 135−137.
(47) LaMattina, J. L.; Taylor, R. L. *J. Org. Chem.* **1981**, *46*, 4179−4182.
(48) Villani, F. J.; Mann, T. A.; Wefer, E. A.; Hannon, J.; Larca, L. L.; Landon, M. J.; Spivak, W.; Vashi, D.; Tozzi, S.; Danko, G.; del Prado, M.; Lutz, M. J. *J. Med. Chem.* **1975**, *18*, 1−8.